Review

Emerging strategies in anticancer combination therapy employing silica-based nanosystems.

Rafael R. Castillo [1,2,3]

María Vallet-Regí [1,2,3]

[1] Departamento de Química en Ciencias Farmacéuticas. Facultad de Farmacia, Universidad Complutense de Madrid, Plaza Ramón y Cajal s/n, 28040, Madrid, Spain.

[2] Centro de Investigación Biomédica en Red—CIBER. 28029, Madrid, Spain.

[3] Instituto de Investigación Sanitaria Hospital 12 de Octubre—imas12. 28041, Madrid, Spain.

Correspondence: María Vallet Regí

Departamento de Química en Ciencias Farmacéuticas.

Facultad de Farmacia, Universidad Complutense de Madrid.

Plaza Ramón y Cajal s/n, 28040, Madrid, Spain.

E-mail: vallet@ucm.es

Keywords: Combination therapy, Ferroptosis, Hypoxia, Immunotherapy, Mesoporous silica nanoparticles.

Abbreviations: AC/DC, Electric current; **ATRA**, *all-trans*-retinoic acid; **BMDCs**, bone-marrow dendritic cells; **βCD**, β-cyclodextrin; **Ce6**, Chlorin e6; **CpG**, an immunostimulant

This article has been accepted for publication and undergone full peer review but has not been through the copyediting, typesetting, pagination and proofreading process, which may lead to differences between this version and the Version of Record. Please cite this article as doi: 10.10002/biot.201900438.

deoxyoligonucleotide; **CPT**, Camptothecin; **DCs**, dendritic cells; **DMONs**, dendritic mesoporous organosilica nanoparticles; **DOX**, Doxorubicin; **ECT**, Electrodynamic chemotherapy; **GM-CSF**, granulocyte-macrophage colony-stimulating factor; **GNT**, Au nanotriangles; **GO**, Glucose oxidase; **GPX4**, Glutathione-dependent peroxidase 4 selenoprotein; **GSH**, Glutathione; **HGP100**, melanoma-derived antigen peptide; **HMSNs**, Hollow mesoporous silica nanoparticles; **HPPL,** hydroperoxide phospholipids; **ICG**, indocyanine green; **IL-2**, Interleukin 2; **IONs**, Iron Oxide Nanoparticles; **LBL**, lipid bilayer; **MHT**, magnetic hyperthermia; **MPLA**, monophosphoryl lipid A; **MSN**, Mesoporous silica nanoparticles; **NI**, Nitroimidazole; **OVA**, Chicken ovalbumin; **P-Dots**, *poly*[2,6-(4,4-bis(2-ethylhexyl)-4*H*-cyclopenta-[2,1-*b*;3,4-*b'*]dithiophene)-*alt*-4,7-(2,1,3-benzothiadiazole)]; **PAB**, 4-phenylazobenzoic acid; **pDAB**, a 4,4'-diazoaniline containing polymer; **PDE**, Photodynamic effect; **PDT**, Photodynamic therapy; **PTE**, Photothermal effect; **PTT**, Photothermal therapy; **PS**, Photosensitizer; **PtNPs**, Pt nanoparticles; **QM**, *p*-quinomethane; **ROS**, Reactive Oxygen Species; **SDE**, Sonodynamic effect; **$TPPS_4$**, *meso*-tetra-(4-sulfonatophenyl)porphyrin; **TPZ**, Tirapazamine; **Trp2**, melanoma-derived antigen peptide; **UCN**, Upconversion nanoparticles; **YM155**, Sepantronium bromide.

Abstract

Combination therapy has emerged as one of the most promising approaches for cancer treatment. However, beyond remotely-triggered therapies that require advanced infrastructures and optimization, new combination therapies based on internally triggered cell-killing effects have also demonstrated promising therapeutic profiles. In this revision, we focus on self-triggered strategies able to improve the therapeutic effect of drug delivery nanosystems. As reviewed, ferroptosis, hypoxia, and immunotherapy show potency enough to treat satisfactorily tumors *in vivo*. However, the interest of combining those with chemotherapeutics, especially with carriers based on mesoporous silica, has provided a new generation of therapeutic nanomedicines with potential enough to achieve complete tumor remission in murine models.

1 Introduction

The development of nanotechnology has permitted the creation of therapeutic nanosystems against many diseases; although, cancer treatment is still the most active research field. This is a consequence of two complementary aspects: first the Enhanced Permeation and Retention effect, a unique physiological feature of solid tumors that provokes bioaccumulation of nanomaterials within solid tumors; and second, the potential to combine in single nanostructures multiple therapeutics and functional components. Several different strategies and possibilities of combination therapy employing nanoparticles as building platforms have been already visited [1–4].

In our previous contribution, we focused on combination therapy employing silica-based nanosystems[1], known for being outstanding platforms for the development of drug delivery nanosystems[5,6]. Therein, we outlined that a combination of drugs was the most immediate strategy to achieve enhanced effects. However, this approach remains a huge challenge, since the co-administration of two potent antitumor compounds may easily cause massive damages and toxic shocks. For this reason, it is generally preferred to combine chemotherapeutics with less toxic, adjuvants capable of increasing the local effect of drugs without boosting the overall toxicity. Those adjuvants could be of different nature and origin. For instance, there have been described successful examples with compounds of biological origins such as peptides, proteins, and nucleic acids[7,8], or of synthetic origins, such as prodrugs, chemical sensitizers, or certain inhibitors.

In addition to those, there are also chemical species able to provoke apoptotic effects upon remote induction. The most representative components are (1) photosensitizers (PS) for photodynamic therapy (PDT), (2) conjugated polymers, certain carbon allotropes, nanometric Au and CuS for photothermal therapy (PTT) or (3) iron oxide nanoparticles (IONs) for magnetic hyperthermia (MHT) respectively[1]. However, although the use of such hybrid species permits to achieve outstanding therapeutic effects, these species also have significant drawbacks and limitations that must be accounted for [9]. For example, IONs are highly biocompatible and offer

a deep and controlled effect, but the high cost of required infrastructure limits its application. On the other side, photochemotherapy is enormously popular, as requires from a cheap and readily available near-infrared laser to activate the plasmonic thermal shock. However, contrary to MHT, the control of the thermal window is much more complex and may lead to the destruction of tumors and surrounding tissues (photoablation) alike, resulting in massive damages.

Another possibility to control the release of chemotherapeutic drugs by remotely triggered stimuli. This permits to obtain more convenient, local, and sustained release form delivery nanoplatforms. Herein, a broad number of stimuli-responsive nanosystems have been reported[10]. For example, ultrasounds, PTT, and MHT have been successfully implemented as remote triggering stimuli[11,12]. However, for delivery purposes, automatic release mechanisms based on chemical responses to the tissue on intracellular microenvironments are of interest, as they permit to exert a highly focalized and unattended therapeutic effect. Regarding those, the most common strategies include: (1) pH shifts, able to cleave acid-labile linkers and to disassemble electrostatically bounded multilayers; (2) Glutathione (GSH) mediated cleavages, able to break disulfide (S-S) bonds throughout a redox process and (3) cleavage by proteolytic processes. Nevertheless, as discussed below, new strategies have been successfully implemented against cancerous cells and microenvironments. For instance, hypoxia-responsive systems or programmed cell death on nutrient-deprived cells, two common situations on tumors, have recently gained attention as anticancer therapies. Herein we will focus on the most recent strategies to achieve this chemical and biological sensitization employing mesoporous silica nanoparticles (MSNs); as summarized in Table 1.

2 Intracellular chemodynamic therapy: Ferroptosis

To avoid the limitations showed by remotely triggered strategies, the scientific community has been searching for new systems able to fight tumors with better accuracy, biocompatibility, and fewer side-effects. One of those emerging strategies is chemodynamic therapy (CDT)[13], which

is based on inducing cellular damage throughout the intracellular generation of reactive oxygen species (ROS).

Ferroptosis is an iron-dependent programmed cell death characterized by the accumulation of hydroperoxide phospholipids (HPPL) within the cell membrane. Unlike apoptosis, which is genetically triggered, ferroptosis is caused by either an excess of iron or a lack of reductive power within the cell[14,15]. Biochemically, intracellular iron can produce a Fenton-like reaction that increases the number of HPPLs within the membranes, disrupting their normal function. On normal cells, this damage could be repaired by the Glutathione-dependent peroxidase 4 selenoprotein (GPX4), the only enzyme from the family able to reduce such HPPLs. Therefore, intracellular ferroptosis could be also triggered by GSH-depletion upon treatments with inhibitors such as Erastin[16] or Neratinib[17]; while on the other hand, this condition could be reversed upon Se supply[18] or ferroptosis inhibitors as liproxstatin-1. Furthermore, ferroptosis has been also reported with other metallic species able to undergo Fenton-like reactions, such as Zn[19], Cu[20], or Mn[21], as will be discussed below.

2.1 Silica-based glutathione depleting systems

As previously outlined, ferroptotic death could be triggered by either a reduction of the activity of the GPX4 repairing protein or by depletion of its substrate. Although GSH has been extensively employed for the development of intracellularly triggered nanosystems[22], its high intracellular concentration and its recovery from NADH makes it very difficult to achieve full depletion with conventional redox-responsive nanosystems. For instance, redox-sensitive MSNs do not exert significant toxicity at high particle concentrations; as demonstrated by the following nanosystems: (1) single-hole hollow MSNs reported by Zhang[23], (2) dendritic mesoporous organosilica nanoparticles (MONs) by Yu[24], or the (3) GSH-disintegrable hollow mesoporous silica nanoparticles (HMSNs) reported by Ghandehari[25] and Shi[26]. For this reason, recent examples aimed at GSH depletion focus on the use of oxidant nanocatalysts and scavengers. Such is the case of the model reported by Ong *et al*., who created an organically-

modified MSNs bearing a pinacol-boronate benzyl carbamate able to release *p*-quinomethane (QM), a GSH scavenger in response to hydrogen peroxide[27]. Herein, the authors also included glucose oxidase onto the particles' surface to provide the necessary H_2O_2 to produce prodrug activation. As a result, this nanosystem increased ROS damage by reducing the levels of bioavailable glucose and NADH together with an efficient GSH scavenging. As a result, augmented oxidative stress could be obtained that can destroy MDA-MB-231 cells.

This depletion strategy has been also successfully employed with different nanosystems. Along this line, Fan *et al*. reported a nanosystem able to deliver intracellularly Chlorin e6 (Ce6) supported onto MnO_2. The system proved to exert a combined Ce6-mediated photodynamic therapy together with MnO_2–mediated depletion of GSH[28]. Similarly, Ma *et al*. reported the use of Cu-cysteine containing nanoparticles able to cause such GSH depletion throughout a Cu-catalyzed generation of hydroxyl radicals[20].

2.2 Catalyst delivery to promote ferroptosis

Previous examples show that iron delivery to tumor areas[29] can induce ferroptosis. This effect was first evidenced in labile nanosystems like IONs and Fe-containing metal-organic frameworks[30]; although have been recently demonstrated with other iron-containing composites[31,32]. Among them, silica-based hybrids[9] have also been demonstrated to be suitable for the induction of ferroptosis in combination with chemotherapeutic drugs, immunostimulants, and targeting elements[33].

For instance, Huo *et al*., employed 40 nm pore dendritic MSNs to load 2nm IONs together with glucose oxidase as H_2O_2 generator[34]. The system proved to generate peroxides *in vitro* which could reduce cell viability on 4T1 and U87 cell lines, especially under mildly acidic conditions. The *in vivo* evaluation of the material provided effective tumor reduction on BALB/c nude mice bearing xenografts and, in some cases, complete tumor remission. On another interesting example, Shieh and coworkers employed iron nanoparticles coated by either porous or non-porous silica to exert ferroptosis onto the OEC-M1 Oral Cancer Cell Line[35]. As expected, the

mesoporous coated hybrids permitted an efficient lysosomal-mediated iron dissolution while the non-porous coating prevented it, leading to a lower therapeutic effect.

However, ferroptosis is not only triggered by iron delivery, as there are iron-containing nanosystems that were not able to exert this effect, while some iron-free nanomaterials exerted ferroptosis in the absence of GPX4 inhibitors. Such is the case of the MRI theragnosis model reported by Fang *et al*., that despite having a Zn doped core-shell ION@MSNs decorated with folic acid and loaded with DOX[36] were not able to exert a synergic cell-killing effect on viability assays. On the opposite case, the α-MSH targeted, Cy5 fluorescent silica nanoparticles (Cornell dots), currently under clinical trials[37], could induce this effect and inhibit tumor progression when evaluated against amino acid-starving melanoma cells[38]. This differentiated effect could, however, be explained by considering the cell culture conditions, which in the second case were driven under starving conditions. Under these circumstances, the lack of nutrients permitted the endogenous iron to induce ferroptosis and hence reduce tumor progression in comparison with untreated mice.

2.3 Combination therapy with nanosystems able to induce ferroptosis

As discussed above, ferroptosis may occur upon depletion of GSH, reduction in the activity of the GPX4 protein, or by augmented metal concentrations. With this idea in mind, several research groups have investigated the potential effect of the simultaneous triggering of pro-ferroptotic pathways. One of those systems, reported by Fei and coworkers, intended to reduce GSH bioavailability by using Sorafenib, an inhibitor of the cystine/glutamate transporter (Xc-), together with a supply of Mn able to promote Fenton-like reaction[39]. The system could induce a deep ferroptosis able to significantly increase the amount of intracellular HPPLs and hence, reduce the cell viability on HepG2 hepatocellular carcinoma cells. Employing a similar strategy, but with another nanoplatform, Cao and coworkers were able to deliver Sorafenib and IONs; which enabled a dual-GSH depletion. Nevertheless, in this model, the presence of IONs allowed them to trigger an additional PTE[40]. The resulting multi-therapeutic nanosystem was able to

induce complete tumor destruction *in vivo* (HCT116) when the three killing effects were combined.

In addition to inhibitors, ferroptosis has been also combined with common anticancer compounds. For example, Dong and coworkers[41] reported a tumor microenvironment responsive nanodevice able to co-deliver DOX together with Fe and Mn cations as ferroptosis promoters. To assemble the system, the authors prepared DOX-loaded MSNs onto which created a Fe^{3+}-doped polydopamine layer. In parallel, the authors prepared folate-tagged Bovine Serum Albumin which was further treated with Mn^{2+} in a biomineralization process. Once both structures were prepared, both were assembled throughout a layer-by-layer electrostatic deposition strategy employing polyethyleneimine as a connecting layer. The resulting system, tested on SMMC-7721 hepatoma cancer cell line, proved to have more killing effect than free DOX or the unloaded system (ferroptosis only), demonstrating that combination therapy, based on ferroptosis, enhances the therapeutic potential of carrier-delivered drugs (Figure 1).

In another interesting contribution, Ling and coworkers developed a targeted nanosystem able to exert a double chemotherapeutic plus ferroptotic effect[42]. To do so, the authors created a hybrid nanosystem based on DOX-loaded porous manganese silicate nanobubbles supported onto arginine-targeted solid SiO_2 nanoparticles. The resulting system was able to internalize into Huh7 liver cancer cells due to the arginine tag and therein, upon the action of GSH and pH decrease, release DOX and Mn^{2+} cations simultaneously. When evaluated *in vivo* the system proved to have a better therapeutic profile than DOX or Mn-containing particles, achieving a significant tumor growth reduction in mice; although unfortunately, without a complete tumor remission.

In another interesting example, Lin *et al*. reported the use of PEGylated MSN@MnO_2 hybrids as carriers for camptothecin (CPT)[43]. Herein, the authors employed CPT-loaded, thiol-capped MSNs able to bind MnO_2 particles; and then, created a PEGylated, pH-sensitive polymeric layer to protect the system from leaks. The evaluation against U87MG cells showed a huge cell viability reduction consequence of the Mn^{2+} and CPT co-delivery, and a promising tumor growth

inhibition when evaluated *in vivo*; although again, without complete tumor destruction. Additional interesting examples of chemodynamic chemotherapy based on ferroptosis are the systems reported by Xue and coworkers[44] who reported the use of structured $CaCO_3$ to co-deliver Fe cations together with DOX and the system by Gao *et al*.[45] who reported a self-assembled structure based on polylysine and polyglutamic acid sequences able to co-deliver Fe ions plus a platinum prodrug.

3 Therapeutic strategies based on hypoxia.

Hypoxia is a hallmark condition that occurs when tissue is deprived of oxygen. It could be caused by either environmental or pathological circumstances: altitude edemas, stroke-affected regions, or at the most internal regions of solid tumors. Regarding cancer, intratumoral hypoxic cells remain a huge problem for current therapies, as those conditions favor the expression of malignant phenotypes and are highly resistant to radio- and chemotherapy[46]. However, hypoxia offers a possibility for the development of promising tumor-specific sensors[47] and therapeutics: (1) hypoxia-triggered prodrugs[48], (2) hypoxia-reversing agents[49], (3) hypoxia-targeted immunotherapy[50], and (4) nanoparticle-based drug delivery systems. Focusing on a mesoporous silica-based nanosystem, there could be found three approaches: (1) anti-hypoxic devices, (2) hypoxia-triggered drug delivery systems, and (3) hypoxia-cleavable prodrug delivery, as outlined in Figure 2.

3.1 Functional nanosystems to revert hypoxic conditions.

As previously outlined, when oxygen supply is not enough to balance homeostasis within the cells, the concentrations of NADH quickly increase to levels able to collapse glycolysis and citrate cycles. Hence, to avoid hypoxia, reference pharmacological treatments employ bioreducible prodrugs able to scavenge the excess of NADH and GSH and able to exert a pharmacological effect once reduced.

Regarding nanotherapeutics, some of those profit from the known ferroptotic and GSH-depleting pathways to treat hypoxia. For instance, in a visionary contribution, Shi and coworkers reported a theragnostic hybrid system based on MnO_2 nanosheets able to reduce hypoxia by reducing GSH levels[51]. The diagnostic feature was achieved with silica-coated upconversion nanoparticles (UCN) which fluorescence was quenched when attached to the MnO_2 layer. Indeed, when the system reached hypoxic areas, monitoring of hypoxia was possible when the MnO_2 was reduced to Mn^{2+} and the fluorescence quenching disappeared. The system also proved to exert tumor growth control by preventing the uncontrolled proliferation of hypoxic areas. Similarly, Hyeon and coworkers designed a dual-therapy nanosystem based on MSNs able to co-deliver a hypoxia-reverting catalyst together with a PS[52]. The nanosystem was assembled employing 2-bromo-2-methyl propionic acid to connect manganese ferrite nanoparticles with amino capped MSNs throughout a pH-sensitive bond. The system demonstrated that the combination of the continuous generation of ROS was able to reduce hypoxia and eventually increase cellular damage. As a result, the system proved to kill U-87MG glioblastoma cells under hypoxic conditions *in vitro* and control tumor progression *in vivo.*

3.2 Functional nanosystems for bioreducible prodrug delivery.

Apart from the nanosystems able to revert hypoxic conditions, other functional models employ bioreducible prodrugs to overcome hypoxia and create double-action nanosystems. For instance, Liu *et al*. designed rattle-like UCN@MSNs to deliver the prodrug tirapazamine (TPZ) to HeLa hypoxic cells and achieve an additional sensitization against radiotherapy[53]. Indeed, the use of this nanosystem in combination with radiotherapy permitted to efficiently destroy hypoxic cells and prevent its evolution towards metastatic phenotypes in both *in vitro* and *in vivo*; as suggested by the Snail and GLU1 proteins expression. Moreover, although not reported, this system enabled remote detection of tumor regions due to the fluorescence of nanoparticles. In another contribution to the topic, Chen *et al*. reported a multilayer-coated MSN to co-deliver the anti-hypoxic TPZ together with a PS[54]. In this system, the initial TPZ-loaded, amino-capped

MSNs were coated with a β-cyclodextrin (βCD) modified hyaluronic acid with a double function: coordinate the PS and provide cell targeting throughout the CD44 receptor. To conclude, the authors closed the system with the $TPPS_4$ porphyrin able to cross-link the βCD rings and coordinate a Gd^{3+} cation to enable remote detection. As a result, the system was able to target and internalize into MCF-7 and SCC-7 cells. Once there, upon pH-mediated disassembly and remote activation of the PS, there was exerted a double killing effect: $TPPS_4$-mediated oxygen depletion plus the pharmacological effect of TPZ. The system was able to destroy almost completely cultured MCF-7 cells when light-activated, with only a 12.4% survival under normoxia and 6.5% under hypoxia (3% O_2). The sequent *in vivo* evaluation demonstrated an outstanding antitumor efficacy that underwent practically complete tumor remission. Moreover, the authors demonstrated adequate biocompatibility for the non-triggered nanosystem, according to typical blood markers: aspartate and alanine transaminases, nitrogen urea, and uric acid, which suggests adequate colloidal stability and trafficking.

Another possibility to exert combination therapy was reported by Wang *et al*., who combined the effect of a bioreducible prodrug with the ROS generation caused by sonodynamic therapy[55]. For this model, the authors employed Ho-doped amino-capped HMSNs able to load TPZ and bind onto the surface both Ce6 and a targeting antibody. The combination of TPZ and Ce6 was able to oxidize the intracellular environment, showing a typical dose-dependent reduction on PC-3 cell viability that was increased when ultrasounds were applied. Regarding *in vivo* studies, the presence of a targeting antibody permitted to effectively target the nanosystem towards the cancerous cells and hence exert a maximal effect, achieving significant tumor destruction.

In addition to the previous examples, PTT has been also successfully combined with hypoxia-triggered prodrugs. In an example reported by Liu and coworkers, the authors employed semiconducting polymer dots as a photothermal dopant and iron-bridged banoxantrone (AQ4N) as a hypoxia-triggered prodrug[56]. To conclude, the system was coated with a pH-sensitive polydopamine layer doped with Mn^{+2} ions to enable magnetic resonance. Like in previous examples, this model provided an outstanding antiproliferative effect on HepG2 cells

due to the combined action of the prodrug and the photothermal effect. Indeed, although not evaluated, the presence of Fe and Mn ions may perhaps increase cell damage caused by ferroptosis upon normoxia recovery. *In vivo* models showed a highly localized thermal effect and significant tumor reduction. In another interesting example, Wang *et al*. reported the use of folate targeted, *Janus* platforms for combined PTT and prodrug delivery[57]. In this model, photoactive Au nanotriangles (GNT) were bounded to MSNs to produce *Janus* GNT-MSNs, which were afterward modified with folic acid and loaded with TPZ. The resulting system was tested on SMMC-7721, Hep3B, HL-7702, and HUVEC cell lines showing significant toxicity but also a nice cell killing profile in the case of loaded particles. The *in vivo* application showed an outstanding therapeutic efficiency, especially enhanced when X-ray radiotherapy was applied together with NIR-mediated PTE and chemotherapy. Unfortunately, despite all the therapeutic arsenal deployed, this system did not achieve complete tumor destruction on murine models. In summary, although both models that combined PTT with bioreducible chemotherapy were not able to destroy tumors completely, such models showed enough therapeutic efficacy to treat certain solid tumors.

3.3 Hypoxia triggered nanosystems based on MSNs.

The third approach for treating hypoxic cells is the use of drug delivery nanosystems bearing bio-reducible coatings or nano-gates. To achieve so, the most employed functional groups are nitro (-NO_2) and diazo (-N=N-), which have shown to react under reductive environments. In the first reported example on the topic, Park and coworkers explored the possibility of a supramolecular assembly between nitroimidazole (NI) and βCD rings to act as nanogates[58]. In this model, the hypoxic conditions were able to reduce the NO_2 group to NH_2, unable to bind the βCD caps, allowing DOX outflow from the mesopores. As a result, cellular assays against SCC-7 cells under hypoxic conditions (0.1%O_2, 5%CO_2) showed viability reductions up to 50%, in concordance with the limited effect of conventional chemotherapeutics on hypoxic cells.

Regarding the examples based on the cleavage of azo containing fragments, Yan *et al*., employed a poly(4,4′-azodianiline) containing polymer as bioreducible coating. The system was completed with Ce6 as cargo and hydrophilic Pluronic F68 hydrophilic outermost layer[59]. As expected, the system did not exert a significant effect unless activated with light (660nm), where the simultaneous depletion of NADH induced by bioreduction and PDT, caused maximal damage. Nevertheless, the absence of potent antiproliferative compounds permitted to obtain only a limited therapeutic effect. In another example by Jang *et al*. an azo-sensitive moiety was employed to build bioreducible nanogates for MSNs[60]. Herein, amino-modified MSNs were first reacted with 4-phenylazobenzoic acid, followed by DOX loading, and finally capped with βCDs. The resulting system proved to have satisfactory drug retention on normoxic, slightly acidic conditions while produced effective DOX release under neutral pH hypoxic conditions. As expected, the system was able to deliver DOX to hypoxic A549 cells, inducing a significant reduction in cell viability. Unfortunately, like in previous examples, no *in vivo* evaluation was reported for these hypoxia-triggered drug delivery nanosystems; which does not allow to foresee yet the potential therapeutic effect of these approaches.

4 Combination therapies based on immune stimulation

Immune stimulation has become too a promising strategy to fight cancer, as it claims to recruit patients' immune systems to destroy tumors. However, to obtain optimal results such activation must occur within the tumor microenvironment[61] to avoid massive damages. With such a premise in mind, it is easy to assume that nanotechnology will play a main role in the development of such treatments, as this technology is one of the few that permits such precise control. In fact, despite its novelty, nanoparticle-based immunotherapy has already become a hot topic according to the number and quality of revisions reported during the last year[62–65]. Unfortunately, typical immunotherapy does not seem to be enough to defeat cancer but may help as an adjuvant on combination therapies (Figure 3). For an extraordinary and visionary revision on the topic, please check the revision authored by Moon and coworkers[66].

Focusing on silica-based nanomaterials,[62] it is important to remark that they have demonstrated an immunostimulant effect. This, first reported by Wang, Tsuji, Ito, and coworkers for HMSNs[67,68] has been also described for multi-shelled dendritic mesoporous organosilica hollow spheres in combination with chicken ovalbumin (OVA)[69] and HMSNs loaded with the TRP2 melanoma-derived antigen peptide[70]. Indeed, Tao and coworkers were the first to explore the potential effect of combined immunostimulants. To do so, the authors explored the behavior of HMSNs[70] loaded with three different immunoactive species: two antigen peptides derived from melanoma and a toll-like receptor (TLR) 4 agonist[71]. In this model, the authors had to tune both internal space and mesopores with different functionalities to achieve a sequential loading of the hydrophobic H2-K^b peptide $TRP2_{180–188}$ (SVYDFFVWL) and the hydrophilic cationic H2-D^b peptide $HGP100_{25–33}$ (KVPRNQWL) at the internal space and mesopores respectively. Finally, to include the TLR4 agonist, the monophosphoryl lipid A (MPLA), the authors employed a lipid coating with a double function: containing the MPLA in between and provide enough retention and colloidal stability. *In vitro*, the resulting protocells induced effective cell maturation of murine bone marrow-derived dendritic cells (BMDCs), as seen by the overexpression of CD86, TNF-α, IFN-γ, IL-12, and IL-4. *In vivo*, the system was able to arrest tumor growth and to stop the creation of melanoma metastatic lymph nodes; demonstrating that even in the absence of chemotherapeutics combination immunotherapy can exert a potent therapeutic effect.

More recently, Kim and coworkers searched for new combination strategies. In a first contribution, the authors took the promising results showed by OVA-loaded nanoparticles[69] and include an additional “danger signal” to enhance the immune response[72]. In this first model, the authors employed large pore MSNs (20-30 nm) to co-load OVA together with an agonist for the TLR9 receptor, a CpG oligonucleotide[73] to promote a strong anticancer vaccination. The treatment with MSNs loaded with OVA and CpG produced increased levels of typical markers from immune induction: $CD4^+$ and $CD8^+$ cells, together with TNF-α, IFN-γ, and IL-12 proteins and the SIINFEKL ($OVA_{257-264}$) antigenic peptide. Unfortunately, despite the

suppression of tumoral growth, complete tumor destruction could not be obtained. Then, to overcome the limitations of this design, these authors decided to explore a more ambitious approach on which an active recruiting and maturation of dendritic cells (DCs) occurred[74]. In this second work, the authors compared three different approaches: (1) the former OVA+CpG@MSNs, (2) the use of mesoporous silica microrods (MSR) to deliver OVA, CpG, and the DC recruiting chemokine GM-CSF (granulocyte-macrophage colony-stimulating factor) and (3) a dual-scale system arisen from the combination of OVA+CpG-loaded MSNs deposited onto a GM-CSF loaded MSR scaffold. All designed formulations were able to reduce tumor progression with efficiency due to DCs' recruitment. However, the last combination provided the highest tumor growth reduction and the survival rate of mice.

Based on the successful combination of OVA and CpG, Yu's group tried to improve the overall therapeutic effect by adding a cell-disrupting effect. In this case, a tetrasulfide containing MONs carrier able to induce GSH-depletion[75]. As a result, this model was able to provoke a metabolic disruption triggered by the intracellular consumption of GSH together with a faster release of both immunostimulants. Consequently, this system was able to exert a significant reduction of cell viability *in vitro* and provided longer survival rates of vaccinated animals.

Apart from the combination of immunostimulants, Kim and coworkers also explored the potential of combined immunotherapy plus PTT[76]. To do so, the authors have employed large pore MSNs to load small AuNPs (1–2nm) suitable for PTE. Finally, to complete the system, the loaded AuNPs were functionalized with thiol-modified CpG and PEG moieties to add the desired immunostimulant feature and to provide enough colloidal stability. According to the data provided, the carried CpG system showed a better immune induction profile than the free oligonucleotide, yielding to higher cancer survival rates. However, the best results were obtained when the dosage of such a nanosystem was combined with a highly controlled PTE (45-50ºC). Under these conditions, there were not produced any tissue/skin damage on treated mice, while there was obtained an improvement in mice survival and tumor control growth.

Apart from previous examples, Kong *et al*. reported the use of lipid-coated HMSNs to co-deliver the tumor sensitizer *all-trans*-retinoic acid (ATRA) together with the anticancer drug DOX and interleukin-2 T-cell growth factor[77]. The system proved to have an important impact on tumor growth reduction, although complete remission was not achieved. Nevertheless, the application *in vivo* of this nanosystem has permitted to drastically reduce the number of lung metastasis caused by the B16F10 melanoma cells. Moreover, in the tumor microenvironment, immunosuppressive cells were depleted while immune effector T cells were activated; two capital aspects to improve cancer's prognosis.

Apart from silica, many other research groups have succeeded in the development of immunochemotherapeutic nanosystems. For instance, Nel and coworkers obtained outstanding results in the treatment of pancreatic ductal adenocarcinoma with oxaliplatin and indoximod, an immunoadjuvant that enhances T-cell activity against cancer, employing nanovesicles[78]. Similarly, Lv and coworkers obtained significant reductions of tumor volumes with a combination of DOX and CpG on a hydrogel formulation against B16 melanoma cells[79].

Another interesting approach was reported by Liu *et al*., who focused on how the degradation of Hyaluronic acid (HA), a major component on tumoral extracellular matrices, could enhance the immune response by facilitating the infiltration of T lymphocytes within the tumors. To do so, the authors prepared a nanosystem based on DOX loaded HMSNs which were first coated with a polyethyleneimine layer and then with a Hyaluronidase throughout sequential electrostatic deposition[80]. As a result, the system was able to mature DCs *in vivo* as suggested by the overexpressed values of interleukins 12p40, 6, and 1β, and increased values of $CD86^{+}$ and $CD11c^{+}$ cells. *In vivo* experiments showed an effective vaccination, as tumors were almost destroyed after 3 weeks of inoculation.

Another interesting combination approach was reported by Zhang *et al*., who studied the possibilities of combining sepantronium bromide (YM155), a survivin inhibitor together with indocyanine green (ICG), a photothermal sensitizer and the anti-CD47 antibody, a promoter of macrophage and T cell-mediated destruction of tumors[81]. To combine all components, the

authors designed two sets of nanoparticles. The first set was enlarged pore MSNs able to co-load and co-delivery ICG and YM155; while the second, antibody-targeted, silica-coated, magnetic nanoparticles, combined antibody immunotherapy with dual (antibody + magnetic) targeting. Independently both nanosystems were able to exert a significant apoptotic effect (about 49% and 76% respectively) on B16F10 cell lines. But when combined, exerted a very effective immune stimulation of DCs, and typical immunoproteins: IL-6, IL12p70, and TNF-α. Unfortunately, *in vivo* tests did not show the expected tumor remission but only a growth arrest; which could be caused by the different kinetics of both particles when administered. Nevertheless, this result demonstrates that even a combination of mild-effect therapeutics could provide interesting overall effects when combined.

5 Electrochemotherapy

Electrochemotherapy (ECT) is a local, nonthermal treatment of tumors that combines typical chemotherapeutic drugs with short and intense electric pulses that transiently and locally, exert a membrane-permeating effect that favors intracellular delivery. The current applications of ECT are mainly intended for skin tumors in veterinary, although are not restricted to those. From a nanomedical point, Liu and coworkers have recently reported a nanosystem able to successfully exert electrochemotherapy[82]. In this system, the authors employed platinum nanoparticles (PtNPs) able to generate cytotoxic ROS under electric current (AC/DC) within the tumor microenvironment. To achieve effective ECT, the authors deposited those PtNPs onto PEGylated, chitosan-coated, DOX-loaded MSNs, which were able to disassemble at lysosomal pH. The resulting nanosystem was able to generate ROS (as determined by methylene blue consumption) only in the presence of electric current, being able to drop cell viability down to *ca.* 30%. As expected, the presence of DOX decreased such viability even more. The evaluation of this system into 4T1 tumor-bearing Balb/C mice showed a significant tumor reduction that even was able to achieve complete tumor destruction, highlighting the potential of the nanotechnological approach of well-known combination therapy (Figure 4).

6 Conclusions

During the past years, combination therapies have been focused on intracellular responsive nanosystems, rather than on remotely triggered nanosystems. This is a direct consequence of the limitations shown by remotely triggered systems which require expensive and complex infrastructures and very precise stimulus application. In the case of the reviewed tumor-triggered therapies, there is also an additional operational advantage: they do not require from a latency period to be self-activated when a threshold is crossed (acidic pH, presence of glutathione, or certain enzymatic cleavages). This is of interest for massive applications as it would not suffer from access restrictions to highly demanded equipment. Moreover, from an application point of view, it is important to remark that best results are obtained in nanosystems able to combine mild apoptotic effects such as immune or chemodynamic therapies rather than on antitumor drug delivery; highlighting the role of those adjuvants therapies in cancer treatment. Also, these emerging approaches still have great potential for improvement. A few examples include fragments to enable remote detection, improve cell-targeting, gain stability against hemolysis, or the action of the immune system.

Acknowledgment

The authors want to acknowledge financial support from the European Research Council ERC-2015-AdG-694160. R.R.C especially acknowledges Centro de Investigación Biomédica en Red (CIBER) for a postdoctoral contract.

Conflict of interest

The authors declare no financial or commercial conflict of interest.

Data Availability Statement.

Not applicable.

Author Contribution

RRC: Conceptualization, Visualization, Writing – Original draft, Writing – Review & Editing.

MVR: Funding acquisition, Project administration, Supervision, Writing – Review & Editing.

7 References

[1] R. R. Castillo, M. Colilla, M. Vallet-Regí, *Expert Opin. Drug Deliv.* **2017**, *14*, 229–243.

[2] S. Gadde, *Medchemcomm* **2015**, *6*, 1916–1929.

[3] S. Bayir, A. Barras, R. Boukherroub, S. Szunerits, L. Raehm, S. Richeter, J.-O. Durand, *Photochem. Photobiol. Sci.* **2018**, *17*, 1651–1674.

[4] Y.-J. Cheng, J.-J. Hu, S.-Y. Qin, A.-Q. Zhang, X.-Z. Zhang, *Biomaterials* **2020**, *232*, 119738.

[5] M. Vallet-Regi, A. Rámila, R. P. del Real, J. Pérez-Pariente, *Chem. Mater.* **2001**, *13*, 308–311.

[6] M. Vallet-Regí, F. Balas, D. Arcos, *Angew. Chem. Int. Ed. Engl.* **2007**, *46*, 7548–7558.

[7] R. R. Castillo, A. Baeza, M. Vallet-Regí, *Biomater. Sci.* **2017**, *5*, 353–377.

[8] R. R. Castillo, D. Lozano, M. Vallet-Regí, *Pharmaceutics* **2020**, *12*, 432

[9] R. R. Castillo, M. Vallet-Regí, *Int. J. Mol. Sci.* **2019**, *20*, 929.

[10] S. Uthaman, K. M. Huh, I.-K. Park, *Biomater. Res.* **2018**, *22*, 22.

[11] Y. Wang, D. S. Kohane, *Nat. Rev. Mater.* **2017**, *2*, 17020.

[12] M. Manzano, M. Vallet-Regí, *Chem. Commun.* **2019**, *55*, 2731–2740.

[13] Z. Tang, Y. Liu, M. He, W. Bu, *Angew. Chemie Int. Ed.* **2019**, *58*, 946–956.

[14] S. J. Dixon, K. M. Lemberg, M. R. Lamprecht, R. Skouta, E. M. Zaitsev, C. E. Gleason, D. N. Patel, A. J. Bauer, A. M. Cantley, W. S. Yang, et al., *Cell* **2012**, *149*, 1060–1072.

[15] J. P. Friedmann Angeli, D. V. Krysko, M. Conrad, *Nat. Rev. Cancer* **2019**, *19*, 405–414.

[16] S. Hao, J. Yu, W. He, Q. Huang, Y. Zhao, B. Liang, S. Zhang, Z. Wen, S. Dong, J. Rao, et al., *Neoplasia* **2017**, *19*, 1022–1032.

[17] A. Nagpal, R. P. Redvers, X. Ling, S. Ayton, M. Fuentes, E. Tavancheh, I. Diala, A. Lalani, S. Loi, S. David, et al., *Breast Cancer Res.* **2019**, *21*, 94.

[18] I. Alim, J. T. Caulfield, Y. Chen, V. Swarup, D. H. Geschwind, E. Ivanova, J. Seravalli, Y. Ai, L. H. Sansing, E. J. Ste.Marie, et al., *Cell* **2019**, *177*, 1262-1279.e25.

[19] C. Zhang, Z. Liu, Y. Zhang, L. Ma, E. Song, Y. Song, *Cell Death Dis.* **2020**, *11*, 183.

[20] B. Ma, S. Wang, F. Liu, S. Zhang, J. Duan, Z. Li, Y. Kong, Y. Sang, H. Liu, W. Bu, et al., *J. Am. Chem. Soc.* **2019**, *141*, 849–857.

[21] S.-M. Hao, J. Qu, Z.-S. Zhu, X.-Y. Zhang, Q.-Q. Wang, Z.-Z. Yu, *Adv. Funct. Mater.* **2016**, *26*, 7334–7342.

[22] M. Vallet-Regí, M. Colilla, I. Izquierdo-Barba, M. Manzano, *Molecules* **2017**, *23*, 47.

[23] D. Wang, Z. Xu, Z. Chen, X. Liu, C. Hou, X. Zhang, H. Zhang, *ACS Appl. Mater. Interfaces* **2014**, *6*, 12600–12608.

[24] Y. Yang, J. Wan, Y. Niu, Z. Gu, J. Zhang, M. Yu, C. Yu, *Chem. Mater.* **2016**, *28*, 9008–9016.

[25] S. P. Hadipour Moghaddam, M. Yazdimamaghani, H. Ghandehari, *J. Control. Release* **2018**, *282*, 62–75.

[26] P. Huang, Y. Chen, H. Lin, L. Yu, L. Zhang, L. Wang, Y. Zhu, J. Shi, *Biomaterials* **2017**, *125*, 23–37.

[27] W. K. Ong, D. Jana, Y. Zhao, *Chem. Commun.* **2019**, *55*, 13374–13377.

[28] H. Fan, G. Yan, Z. Zhao, X. Hu, W. Zhang, H. Liu, X. Fu, T. Fu, X.-B. Zhang, W. Tan, *Angew. Chemie Int. Ed.* **2016**, *55*, 5477–5482.

[29] M. Liu, B. Liu, Q. Liu, K. Du, Z. Wang, N. He, *Coord. Chem. Rev.* **2019**, *382*, 160–180.

[30] D. W. Zheng, Q. Lei, J. Y. Zhu, J. X. Fan, C. X. Li, C. Li, Z. Xu, S. X. Cheng, X. Z. Zhang, *Nano Lett.* **2017**, *17*, 284–291.

[31] W. Bao, X. Liu, Y. Lv, G.-H. Lu, F. Li, F. Zhang, B. Liu, D. Li, W. Wei, Y. Li, *ACS Nano* **2019**, *13*, 260–273.

[32] X. Yao, P. Yang, Z. Jin, Q. Jiang, R. Guo, R. Xie, Q. He, W. Yang, *Biomaterials* **2019**, *197*, 268–283.

[33] X. Shan, S. Li, B. Sun, Q. Chen, J. Sun, Z. He, C. Luo, *J. Control. Release* **2020**, *319*, 322–332.

[34] M. Huo, L. Wang, Y. Chen, J. Shi, *Nat. Commun.* **2017**, *8*, 357.

[35] L.-X. Yang, Y.-N. Wu, P.-W. Wang, W.-C. Su, D.-B. Shieh, *Int. J. Mol. Sci.* **2019**, *20*, 4336.

[36] W. Fang, W. Zhu, H. Chen, H. Zhang, S. Hong, W. Wei, T. Zhao, *ACS Appl. Bio Mater.* **2020**, *3*, 1690–1697.

[37] A. C. Anselmo, S. Mitragotri, *Bioeng. Transl. Med.* **2019**, *4*, 1–16.

[38] S. E. Kim, L. Zhang, K. Ma, M. Riegman, F. Chen, I. Ingold, M. Conrad, M. Z. Turker, M. Gao, X. Jiang, et al., *Nat. Nanotechnol.* **2016**, *11*, 977–985.

[39] H. Tang, D. Chen, C. Li, C. Zheng, X. Wu, Y. Zhang, Q. Song, W. Fei, *Int. J. Pharm.* **2019**, *572*, 118782.

[40] Q. Guan, R. Guo, S. Huang, F. Zhang, J. Liu, Z. Wang, X. Yang, X. Shuai, Z. Cao, *J. Control. Release* **2020**, *320*, 392–403.

[41] Y. Zhang, O. Eltayeb, Y. Meng, G. Zhang, Y. Zhang, S. Shuang, C. Dong, *New J. Chem.* **2020**, *44*, 2578–2586.

[42] S. Wang, F. Li, R. Qiao, X. Hu, H. Liao, L. Chen, J. Wu, H. Wu, M. Zhao, J. Liu, et al., *ACS Nano* **2018**, *12*, 12380–12392.

[43] L.-S. Lin, J. Song, L. Song, K. Ke, Y. Liu, Z. Zhou, Z. Shen, J. Li, Z. Yang, W. Tang, et al., *Angew. Chemie* **2018**, *130*, 4996–5000.

[44] C.-C. Xue, M.-H. Li, Y. Zhao, J. Zhou, Y. Hu, K.-Y. Cai, Y. Zhao, S.-H. Yu, Z. Luo, *Sci. Adv.* **2020**, *6*, eaax1346.

[45] Z. Gao, T. He, P. Zhang, X. Li, Y. Zhang, J. Lin, J. Hao, P. Huang, J. Cui, *ACS Appl. Mater. Interfaces* **2020**, *12*, 20271–20280.

[46] J. M. Brown, W. R. Wilson, *Nat. Rev. Cancer* **2004**, *4*, 437–447.

[47] J. Liu, J. Liang, C. Wu, Y. Zhao, *Anal. Chem.* **2019**, *91*, 6902–6909.

[48] L. Spiegelberg, R. Houben, R. Niemans, D. de Ruysscher, A. Yaromina, J. Theys, C. P. Guise, J. B. Smaill, A. V. Patterson, P. Lambin, et al., *Clin. Transl. Radiat. Oncol.* **2019**, *15*, 62–69.

[49] K. Graham, E. Unger, *Int. J. Nanomedicine* **2018**, *13*, 6049–6058.

[50] S. Chouaib, M. Z. Noman, K. Kosmatopoulos, M. A. Curran, *Oncogene* **2017**, *36*, 439–445.

[51] W. Fan, W. Bu, B. Shen, Q. He, Z. Cui, Y. Liu, X. Zheng, K. Zhao, J. Shi, *Adv. Mater.* **2015**, *27*, 4155–4161.

[52] J. Kim, H. R. Cho, H. Jeon, D. Kim, C. Song, N. Lee, S. H. Choi, T. Hyeon, *J. Am. Chem. Soc.* **2017**, *139*, 10992–10995.

[53] Y. Liu, Y. Liu, W. Bu, Q. Xiao, Y. Sun, K. Zhao, W. Fan, J. Liu, J. Shi, *Biomaterials* **2015**, *49*, 1–8.

[54] W.-H. Chen, G.-F. Luo, W.-X. Qiu, Q. Lei, L.-H. Liu, S.-B. Wang, X.-Z. Zhang, *Biomaterials* **2017**, *117*, 54–65.

[55] Y. Wang, Y. Liu, H. Wu, J. Zhang, Q. Tian, S. Yang, *Adv. Funct. Mater.* **2019**, *29*, 1805764.

[56] D. Zhang, Z. Cai, N. Liao, S. Lan, M. Wu, H. Sun, Z. Wei, J. Li, X. Liu, *Chem. Sci.* **2018**, *9*, 7390–7399.

[57] Z. Wang, Z. M. Chang, D. Shao, F. Zhang, F. Chen, L. Li, M. F. Ge, R. Hu, X. Zheng, Y. Wang, et al., *ACS Appl. Mater. Interfaces* **2019**, *11*, 34755–34765.

[58] S. Khatoon, H. Han, J. Jeon, N. Rao, D.-W. Jeong, M. Ikram, T. Yasin, G.-R. Yi, J. Park, *Polymers (Basel).* **2018**, *10*, 390.

[59] Q. Yan, X. Guo, X. Huang, X. Meng, F. Liu, P. Dai, Z. Wang, Y. Zhao, *ACS Appl. Mater. Interfaces* **2019**, *11*, 24377–24385.

[60] E. H. Jang, G. L. Kim, M. G. Park, M. K. Shim, J.-H. Kim, *J. Drug Deliv. Sci. Technol.* **2020**, *56*, 101543.

[61] L. Gu, D. J. Mooney, *Nat. Rev. Cancer* **2016**, *16*, 56–66.

[62] T. L. Nguyen, Y. Choi, J. Kim, *Adv. Mater.* **2018**, 1803953.

[63] C. W. Shields, L. L. W. Wang, M. A. Evans, S. Mitragotri, *Adv. Mater.* **2019**, 1901633.

[64] K. L. Hess, I. L. Medintz, C. M. Jewell, *Nano Today* **2019**, *27*, 73–98.

[65] C. Song, F. Li, S. Wang, J. Wang, W. Wei, G. Ma, *Adv. Ther.* **2019**, 1900115.

[66] J. Nam, S. Son, K. S. Park, W. Zou, L. D. Shea, J. J. Moon, *Nat. Rev. Mater.* **2019**, *4*, 398–414.

[67] X. Wang, X. Li, A. Ito, K. Yoshiyuki, Y. Sogo, Y. Watanabe, A. Yamazaki, T. Ohno, N. M. Tsuji, *Small* **2016**, *12*, 3510–3515.

[68] X. Wang, X. Li, K. Yoshiyuki, Y. Watanabe, Y. Sogo, T. Ohno, N. M. Tsuji, A. Ito, *Adv. Healthc. Mater.* **2016**, *5*, 1169–1176.

[69] Y. Yang, Y. Lu, P. L. Abbaraju, J. Zhang, M. Zhang, G. Xiang, C. Yu, *Angew. Chemie - Int. Ed.* **2017**, *56*, 8446–8450.

[70] Q. Liu, Y. Zhou, M. Li, L. Zhao, J. Ren, D. Li, Z. Tan, K. Wang, H. Li, M. Hussain, et al., *ACS Appl. Mater. Interfaces* **2019**, *11*, 47798–47809.

[71] J. Xie, C. Yang, Q. Liu, J. Li, R. Liang, C. Shen, Y. Zhang, K. Wang, L. Liu, K. Shezad, et al., *Small* **2017**, *13*, 1701741.

[72] B. G. Cha, J. H. Jeong, J. Kim, *ACS Cent. Sci.* **2018**, *4*, 484–492.

[73] D. M. Klinman, *Nat. Rev. Immunol.* **2004**, *4*, 249–259.

[74] T. L. Nguyen, B. G. Cha, Y. Choi, J. Im, J. Kim, *Biomaterials* **2020**, *239*, 119859.

[75] Y. Lu, Y. Yang, Z. Gu, J. Zhang, H. Song, G. Xiang, C. Yu, *Biomaterials* **2018**, *175*, 82–92.

[76] C. Ong, B. G. Cha, J. Kim, *ACS Appl. Bio Mater.* **2019**, *2*, 3630–3638.

[77] M. Kong, J. Tang, Q. Qiao, T. Wu, Y. Qi, S. Tan, X. Gao, Z. Zhang, *Theranostics* **2017**, *7*, 3276–3292.

[78] J. Lu, X. Liu, Y.-P. Liao, F. Salazar, B. Sun, W. Jiang, C. H. Chang, J. Jiang, X. Wang, A. M. Wu, et al., *Nat. Commun.* **2017**, *8*, 1811.

[79] X. Dong, A. Yang, Y. Bai, D. Kong, F. Lv, *Biomaterials* **2020**, *230*, 119659.

[80] Q. Liu, Y. Sun, X. Yin, J. Li, J. Xie, M. Xie, K. Wang, S. Wu, Y. Li, M. Hussain, et al., *ACS Appl. Bio Mater.* **2020**, *3*, 3378–3389.

[81] Y. Zhang, H. Chen, H. Wang, T. Wang, H. Pan, W. Ji, J. Chang, *Chem. Eng. J.* **2020**, *380*, 122472.

[82] T. Gu, T. Chen, L. Cheng, X. Li, G. Han, Z. Liu, *Nano Res.* **2020**, *13*, 2209–2215.

Table 1. Novel nanosystems suitable for combined therapy. Chemical species between square brackets indicate therapeutic role and location for round shaped brackets in multicomponent assemblies.

Nanocarrier system	*Primary therapeutic*	*Secondary therapeutic*	*Responsive element*	*Action mechanisms*	*In vitro/ In vivo*	*Ref.*
Silica-based glutathione depleting systems.						
MSNs	QM	GO	H_2O_2	Dual GSH depletion	MDA-MB-231 None	[27]
Catalyst delivery to promote ferroptosis.						
Dendritic MSNs	Fe_3O_4 NPs GO	None	None	Fe-ferroptosis Glucose depletion	4T1, U87 Mice	[34]
Fe@MSNs	Fe	None	pH	Fe-ferroptosis	OEC-M1 None	[35]
Cornell dots	None	None	None	Unknown	M21 Mice	[38]
Nanosystems for combined ferroptosis and chemotherapy						
Mn-doped MSNs	Mn(II)	Sorafenib	GSH	Mn-ferroptosis GSH-depletion	HepG2 None	[39]
MSNs	Fe(III) Mn(IV)	DOX	pH	Fe/Mn Ferroptosis Chemotherapy	SMMC-7721 None	[41]
MSN@$MnSO_4$	Mn(II)	DOX	pH	Mn-ferroptosis Chemotherapy	Huh7 Mice	[42]
MSN@MnO_2	Mn(IV)	CPT	pH	Mn-ferroptosis Chemotherapy	U87MG Mice	[43]
Combination therapy based on hypoxia triggered prodrug delivery						
UCN@HMSNs	TPZ	Radiotherapy	UCN	Prodrug delivery	Hela Mice	[53]
MSNs	TPZ	$TPPS_4$	Gd(III) (T_1 MRI)	Prodrug delivery PDE	COS7, MCF-7, SCC-7 Mice	[54]
HMSNs	TPZ	Ce6	Ho(III) (T_2 MRI)	Prodrug delivery SDE	PC-3 Mice	[55]
MSNs	AQ4N	P-Dots	Mn(II) (T_2 MRI)	Prodrug delivery PTE	HepG2 Mice	[56]
Janus GNT-MSNs	TPZ	GNT		Prodrug delivery PTE	SMMC-7721 HL-7702 Mice	[57]
Hypoxia-triggered drug delivery						
MSNs	DOX	---	NI βCD	-NO_2 reduction βCD cleavage	SCC-7 None	[58]
MSNs	Ce6	---	pDAB	Azo-reduction Photoexcitation	MCF-7 None	[59]

MSNs	DOX	---	PAB-βCD	Azo-reduction βCD cleavage	A549 None	[60]
Combination immunotherapy						
HMSNs	OVA	---	[HMSNs]	None	E.G7-OVA, LCC, Mice	[67,68]
MSOSNs	OVA	---	[MSOSNs]	None	RAW264.7 Mice	[69]
HMSNs	TRP2	---	[HMSNs]	None	DCs 2.4, BMDCs Mice	[70]
HMSNs@LBL	TRP2	HGP100	MPLA	Lipid-mediated	BMDCs Mice	[71]
HMSNs	OVA	CpG	---	None	BMDCs Mice	[72]
HMSN@MSRs	OVA (@HMSNs)	CpG (@HMSNs)	GM-CSF (@MSRs)	None	BMDCs Mice	[74]
DMONs	OVA	CpG	-S_4- moiety	GSH-mediated cleavage	B16OVA Mice	[75]
Au@MSNs	CpG	AuNPs	---	PTE	BMDCs Mice	[76]
MSN@LBL	DOX	IL-2	ATRA	None	B16F10 Mice	[77]
HMSNs	DOX	HAase	---	pH mediated disassembly	B16F10 Mice	[80]
MNP@nSiO_2 MSNs	anti-CD47 (MNP@nSiO_2)	YM155 (@MSNs)	ICG (@MSNs)	None NIR	B16F10 Mice	[81]
Electrodynamic chemotherapy						
MSNs	DOX	PtNPs		ECT	4T1 Mice	[82]

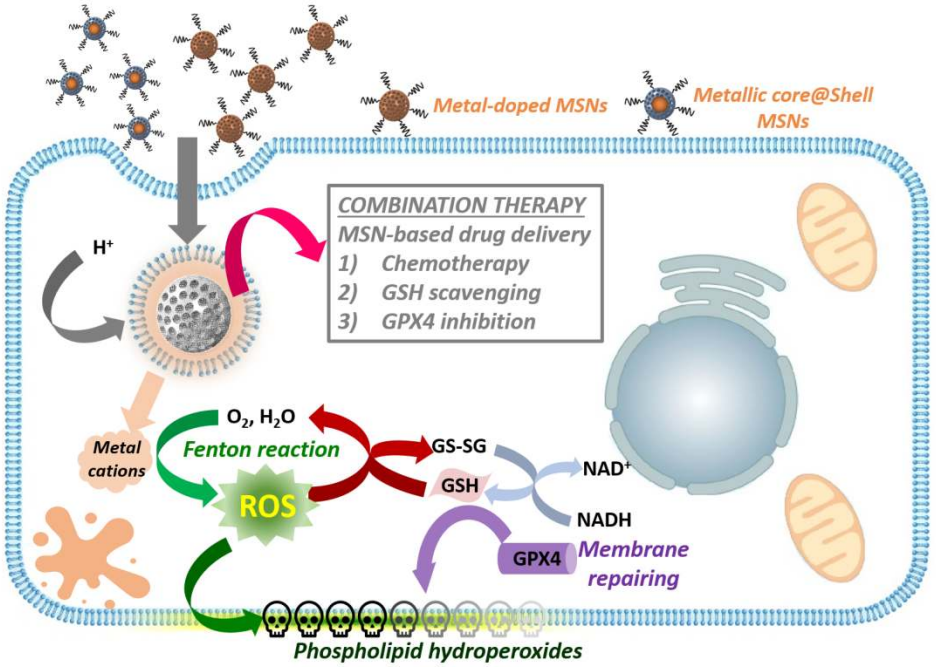

Figure 1. Action pathways on ferroptosis inductive nanosystems for combined chemodynamic chemotherapy.

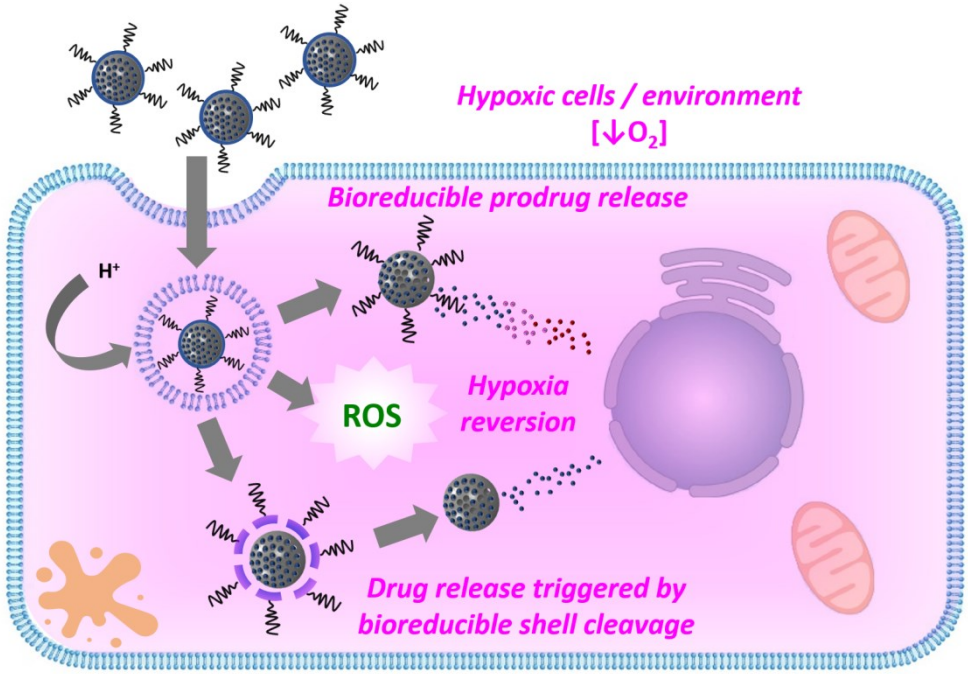

Figure 2. Therapeutic strategies to treat hypoxic cancerous cells. Combination therapies arise when nanosystems are capable of reverting hypoxia and exert an additional therapeutic effect.

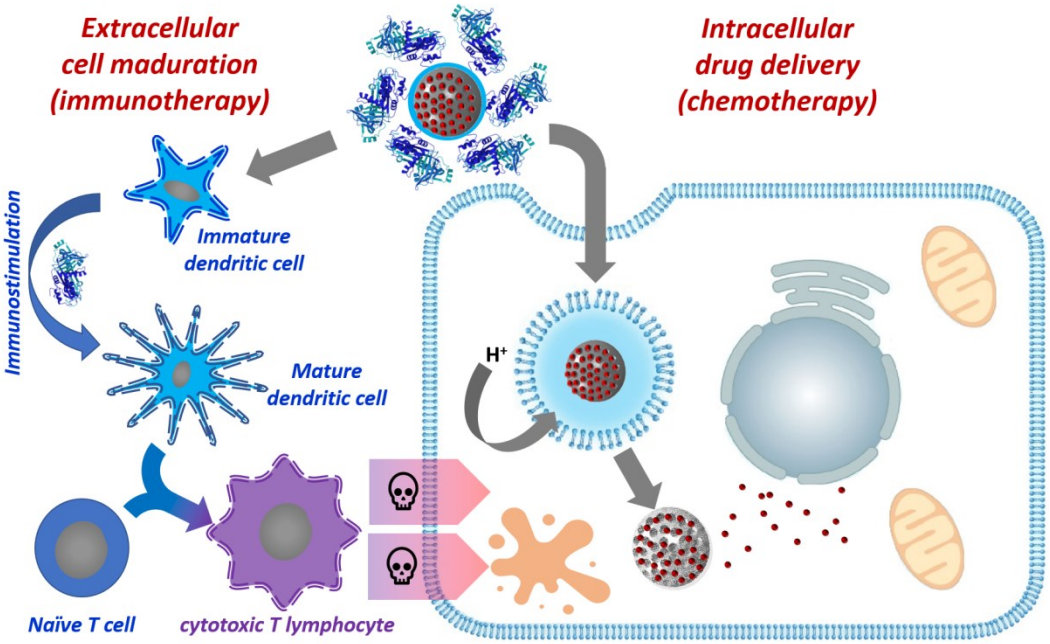

Figure 3. Typical design and action mechanism of immunochemotherapeutic nanodevices.

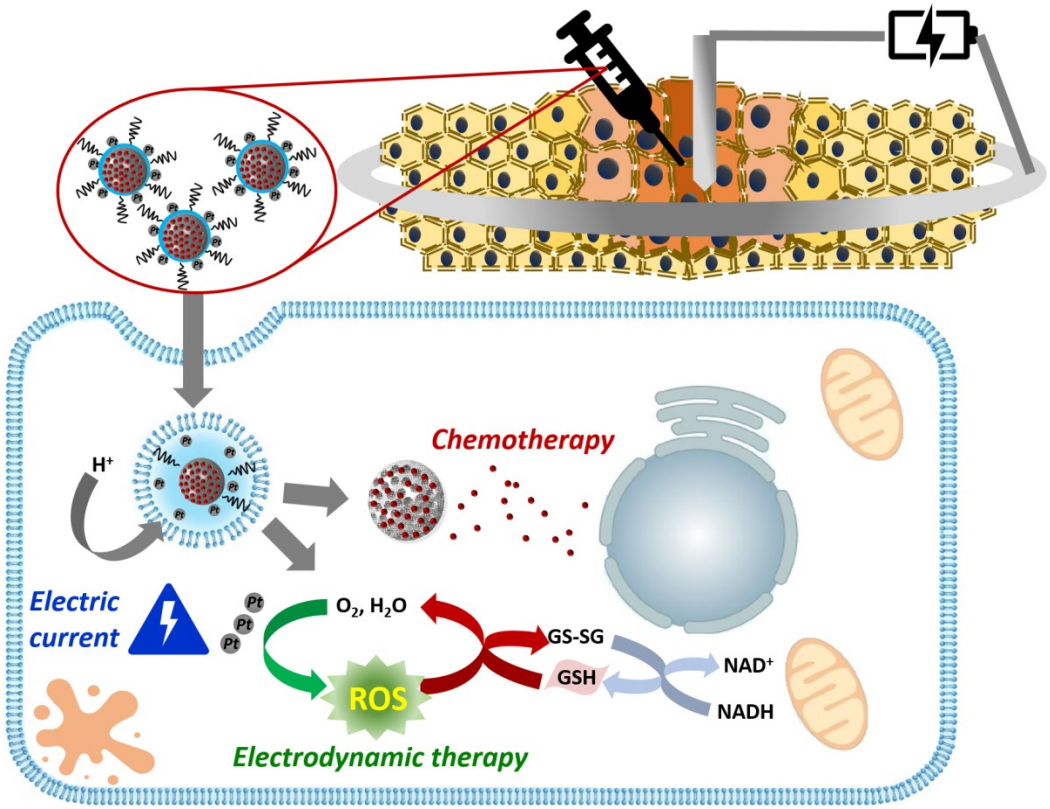

Figure 4. Schematic action mechanism for electrodynamic chemotherapy combination nanotherapy. Herein Pt nanoparticles can produce ROS upon excitation with an electric current.

About the authors

Professor María Vallet-Regí is a Spanish chemist, scientist, and Professor at Universidad Complutense de Madrid, Spain. She is recognized as a pioneer in the field of ceramic materials applied to medicine. She was the pioneer who suggested introducing drugs into the pores of mesoporous silica materials, which inspired thousands of publications worldwide involving mesoporous silica nanoparticles for drug delivery. She is a Highly Cited Researcher 2018 (Clarivate Analytics). Her publications have been cited over 45.900 times and her h-index is 101. Prof. Vallet-Regí has been awarded many important International prizes. She has recently obtained an ERC Advanced Grant entitled “Polyvalent mesoporous nanosystem for bone diseases”

Rafael Castillo, born in Spain in 1979, studied chemistry at Universidad de Alcalá, where he gets his Ph.D. in 2009. After two postdocs at Centre National de la Recherche Scientifique and the Autonomous University of Madrid, he joined the Department Pharmaceutical Sciences at the Complutense University of Madrid in which in collaboration with prof. Vallet-Regí, he has focused his research on the use of silica mesoporous nanoparticles for the development of functional nanosystems suitable for drug delivery and biomedical applications.

Graphical abstract

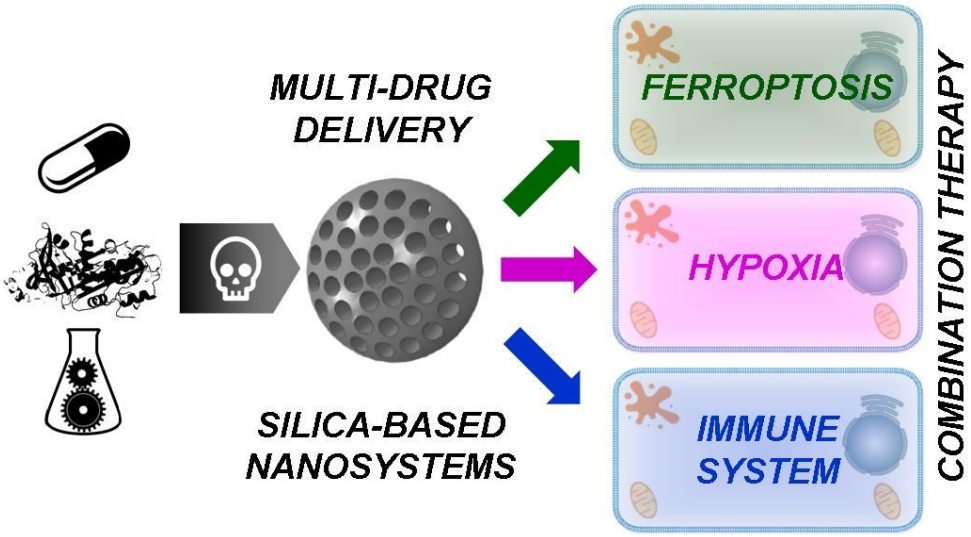

Nanosystems have emerged as a powerful tool for the delivery of drug combinations. Herein we focus on the possibilities of mesoporous silica-based nanosystems for combining chemotherapy with novel internally triggered cell killing effects: ferroptosis, hypoxia and immunotherapy.